Ellipsometry as a Probe of Crystallization in Binary Blends of a Sphere-Forming Diblock Copolymer

Jessica L. Carvalho,[1,2] Michael E. Somers,[1,2] Kari Dalnoki-Veress[1,2]

[1]Department of Physics and Astronomy, McMaster University, Hamilton, Ontario, Canada

[2]Brockhouse Institute for Materials Research, McMaster University, Hamilton, Ontario, Canada

Correspondence to: K. Dalnoki-Veress (E-mail: dalnoki@mcmaster.ca)

Received 23 November 2010; revised 20 January 2011; accepted 22 February 2011; published online 2011
DOI: 10.1002/polb.22242

ABSTRACT: Ellipsometry is used to measure the crystallization and melting temperature of a bidisperse blend of a crystalline-amorphous diblock copolymer. Binary blends of sphere-forming poly(butadiene-ethylene oxide) (PB-PEO) of two different molecular weights are prepared. The two PB-PEO diblocks that are used share the same amorphous majority PB block length but different crystalline PEO minority block length. As the concentration of higher molecular weight diblock in the blend is increased, the size of the PEO spherical domains swell, providing access to the full range of domain sizes between the limits of the two neat diblock components. The change in domain size is consistent with a monotonic change in both the crystallization and melting temperatures. © 2011 Wiley Periodicals, Inc. J Polym Sci Part B: Polym Phys 49: 712–716, 2011

KEYWORDS: block copolymers; crystallization; nucleation

INTRODUCTION Studying the initial stage of crystallization, the birth of a crystal nucleus, remains experimentally challenging because of the dominance of defect driven nucleation in bulk systems. The use of small, isolated domains of crystalline material has proven to be invaluable to this research effort. In typical bulk samples, the nucleation rate is convoluted with the growth rate. However, by subdividing the bulk into many small domains, nucleation statistics become accessible. Small domains ranging from micrometers to nanometers in size can ensure that it is possible for the domains to outnumber the defects in the system. Thus, homogenous nucleation, rather than defect driven heterogenous nucleation, becomes the dominant mechanism. Furthermore, because large supercooling is typically required to overcome the high activation barrier associated with homogenous nucleation, once a nucleation event occurs the crystal grows rapidly in comparison to the rate at which nuclei appear. For this reason, there is separation of timescales and the overall crystallization rate is a direct probe of the nucleation rate. Measurements of this type have typically been carried out using small crystallizable droplets that were phase-separated in an amorphous matrix,[1–7] droplets dewetted on some substrate,[8–12] or using phase separated block copolymers which provide an ideal system for creating isolated nanoscale domains.[13–21]

Here we focus on crystalline-amorphous (C-A) diblocks. If the minority block is chosen to be crystalline and a suitable amorphous polymer is chosen for the majority block such that the interblock segregation strength is large enough, crystallization can be contained within the phase-separated domains. The dimensions of the phase-separated structure depend on the volume fraction of the minority block, so different domain sizes can be obtained by adjusting this volume fraction. The benefit of using phase separated block copolymers is the vast number of nanoscale, defect-free, monodisperse, compartments that self-assemble within a single sample. In addition, the effects of one-, two-, and three-dimensional confinement may be explored by investigating lamella, cylinder, or sphere forming C-A diblocks. Techniques such as differential scanning calorimetry (DSC), scattering, and ellipsometry can easily follow the simultaneous crystallization of the domains as the sample is cooled. The monodisperse domains which self-assemble from diblock copolymers which makes them so ideally suited for these measurement techniques, can also be a drawback: investigating different domain sizes requires the synthesis of a new diblock, making such important studies challenging and time consuming.[22]

We investigate a simple approach to tailoring the domain-size of sphere-forming diblocks and measuring the crystallization and melting temperatures. By blending two C-A diblocks of the same composition but differing molecular weight, a range of length scales can be accessed. The phase separated morphology of binary diblock blends has been extensively studied.[22–32] Much of this work has focused on blends of lamellae forming diblocks. It has been shown that the domain spacing depends on the average molecular weight of the blends. Some of these studies have investigated the effect of crystallization within

blended diblock phases.[27,28,32] The C-A diblock investigated here is an asymmetric sphere-forming system. We consider the simple scenario where a fixed length is maintained for the amorphous majority blocks, and the minority crystallizable block lengths are chosen to be different. The resultant domain sizes can be monotonically adjusted between that of two pure diblocks simply by changing the composition of the blended samples. We monitor the crystallization and melting temperatures of the domains as a function of blend composition. Thus, blending the two C-A diblocks is a simple way to expand the range of domain sizes accessible for crystallization studies without the need for extensive polymer synthesis.

EXPERIMENT

Blends of two sphere-forming 1-4 addition poly(butadiene-b-ethylene oxide) (PB-PEO) diblock copolymers were investigated for these studies (see Table 1 for polymer details). For all three C-A diblocks, the A-block length was kept constant with number averaged molecular weight, $M_n = 26$ kg/mol, while the C-block was $M_n = 3.5$, 4.5, and 7.5 kg/mol (polydispersity index, PI = 1.06). The three diblocks will be referred to as 3.5 k, 4.5 k, and 7.5 k. The two extremes, 3.5 k and 7.5 k were blended to explore intermediate domain sizes, while the 4.5 k system provides a monodisperse unblended case for comparison with the 3.5 k/7.5 k mixtures. We have estimated the radius of the PEO spheres in melts of pure 3.5 k, 4.5 k, and 7.5 k diblock to be approximately 5 nm, 8 nm, and 14 nm based on strong-stretching theory (The estimate is based on strong-stretching theory for the minority domain size as described by Matsen and Bates,[33] while experimental parameters for the sphere size and volume fraction were measured for the equivalent system by Huang et al.[27]). As discussed by Huang et al.,[27] polybutadiene homopolymer (h-PB) was blended, 20% by mass, with the diblocks to inhibit domain coalescence upon crystallization ($M_w = 1.9$ kg/mol, PI = 1.08). The addition of this h-PB ensures that the crystallizable domains are spatially segregated so that crystallization in one domain is independent from a neighboring domain. All polymer was obtained from Polymer Source, Dorval, Canada.

Blends of the 7.5 k and 3.5 k diblocks were dissolved with h-PB in toluene with a total polymer concentration of about 3% by mass. Since the mass fraction of h-PB is fixed at 0.2 of the total polymer concentration and is present only to segregate the PEO domains, we use the mass fraction, ϕ, to denote the fraction of 7.5 k diblock of the total diblock polymer. For example, $\phi = 0$ represents a film that consists of 3.5 k diblock copolymer with 5 nm domains, while a film prepared with 7.5 k diblock will have domains with radius 14 nm and $\phi = 1$. The monodisperse 4.5 k diblock was also dissolved in toluene with h-PB for comparison to the bidisperse blends. Films were prepared by spincoating the solutions onto clean silicon substrates, resulting in uniform films with $h \sim 160$ nm. Films were vacuum annealed (10^{-6} Torr) for at least 24 h at 90 °C. This annealing temperature is above the melting temperature for PEO ($T_m \sim 65$ °C) and the glass-transition temperature of PB ($T_g < -40$ °C),[34] but well below the order-disorder transition temperature of the diblock (<220 °C).[35] The annealing treatment ensured the films were well ordered, resulting in PEO minority spheres embedded in a PB matrix. Atomic force microscopy (AFM) was used to verify that such samples were indeed ordered with spherical domains. After annealing, the samples were transferred to the ellipsometer. Cooling and heating of the samples was carried out at 2 °C/ min.

TABLE 1 Polymer Details: The Number Averaged Molecular Weights for the PEO and PB Blocks, the Polydispersity Index, and the Domain Radius

M_N^{PEO} (kg/mol)	M_N^{PB} (kg/mol)	PI	Radius (nm)
3.5	26	1.06	7.5
4.5	26	1.06	8.5
7.5	26	1.06	13.5

While previous measurements of nano-confined crystallization in diblocks has typically been carried out with DSC,[14,15,17,19,21] here we use ellipsometry to probe crystallization.[10,36–38] Ellipsometry exploits the fact that linearly polarized light emerges elliptically polarized when reflected from a film covered substrate to obtain the thickness and index of refraction of a film.[36] Ellipsometry measurements were carried out on a custom-built, single-wavelength (633 nm) ellipsometer. Though many approaches to ellipsometry are employed and could work equally well for the studies described, here we use a self-nulling ellipsometer. In this mode, circularly polarized light is passed through a polarizer and quarter wave plate such that when the polarizer is rotated to angle P, the elliptically polarized light produced is linearly polarized after reflection from the sample. A second polarizer, called the analyzer, is then rotated to null the light at the detector, at an angle A. The angles P and A can be related to the film thickness, h, and refractive index, n, using standard equations of ellipsometry.[36] Though ellipsometry is much more sensitive, AFM was used on some of the samples to verify the ellipsometry thickness results. Here the angle of incidence was set to 50° and a set of ellipsometric angles (P, A) collected every ~12 s, corresponding to a measurement every ~0.4 °C. The ellipsometer was equipped with a heating stage (a modified Linkam THMS 600, United Kingdom) and flushed with dry nitrogen for performing temperature dependent measurements of $h(T)$ and $n(T)$.

RESULTS AND DISCUSSION

In previous work, we have demonstrated the ability to study crystallization within minority domains of thin sphere-forming diblock films using ellipsometry.[37] Ellipsometry is a technique that is complementary to more standard tools like DSC and affords a few advantages. While the ability to work at very slow heating and cooling rates can be useful, perhaps the main advantage is the ability to measure crystallization in tiny volumes of $\sim 10^{-10}$ L. Previously we were able to measure differences in crystallization temperatures for two PB-PEO diblocks of identical PB block length but different minority PEO length. As expected, the sample with the larger PEO block

length displayed a higher crystallization temperature than the sample with the shorter PEO block length. This is consistent with the fact that the smaller molecular weight results in phase-separated spherical domains of smaller radius and the probability of a nucleation event scales with the volume of the domain.[10] Thus, greater supercooling is required to create a crystal nucleus as the domain volume decreases. The equilibrium domain size of a particular diblock is the result of the drive to minimize the amount of unfavorable interface between the two blocks while at the same time minimizing unfavorable chain stretching within the individual chains.[39] By blending two diblocks of the same PB length but different PEO length, we vary the domain size between the extreme values of the unblended diblocks. Since the crystallization temperature, T_c, can be interpreted as a metric of the size of domains,[10] we can correlate T_c to the blend concentration, ϕ.

The results of a typical ellipsometry experiment can be seen in Figure 1. The example shown is for a film with $\phi = 0.85$ (i.e., 85% 7.5 k and 15% 3.5 k diblock). The measured P and A angles are given in Figure 1(a,b) as a function of temperature. Assuming a uniform film one can convert the unique angles P and A to values of film thickness, h, and refractive index, n, using standard equations of ellipsometry[36] [Fig. 1(c,d)]. We note that the assumption of a uniform film is an excellent approximation even for phase-separated diblock films for two reasons: (1) The footprint of the laser is about 1 mm × 3 mm with $h = 160$ nm, a volume that averages over approximately 10^{10} domains. (2) The wavelength of light is about two orders of magnitude larger than the size of a domain. After annealing at 80 °C for a few minutes, the film was cooled at a fixed rate of 2 °C/ min. Once the film reached a temperature below −20 °C, a rapid contraction took place as the PEO domains crystallised. The nucleation events, followed by the rapid crystallization of the spherical domains, result in an easily measurable contraction which is reflected in the sudden decrease in films thickness and concurrent increase in the index of refraction. Cooling was continued to −40 °C. The linearity of the curve in the plots of h and n following crystallization indicates that crystallization is completed within a narrow range of temperatures around −23 °C. After being held at −40 °C for 10 min, the film was heated at 2 °C/ min. Just above 50 °C, a rapid expansion of the film was measured, consistent with the expected melting temperature for PEO domains crystallised at this temperature. The film was further heated to a final temperature of 80 °C. It can be seen that there is almost no drift in the measured data since the heating and cooling data above the melting transition lie directly on top of each other. The midpoint of the crystallization and melting transitions are used to identify T_c and T_m (the midpoint was identified by evaluating the point of inflection in the data). We note that the slope, dh/dT, of the cooling data prior to crystallization is steeper than the slope upon heating the film with crystalline domains. The difference in the slope is simply the result of the difference in the expansion coefficient of the melt and crystalline PEO. The sensitivity and precision of the ellipsometry technique for following these phase changes, and expansion coefficients in thin films is evidenced by the quality of the measured curves

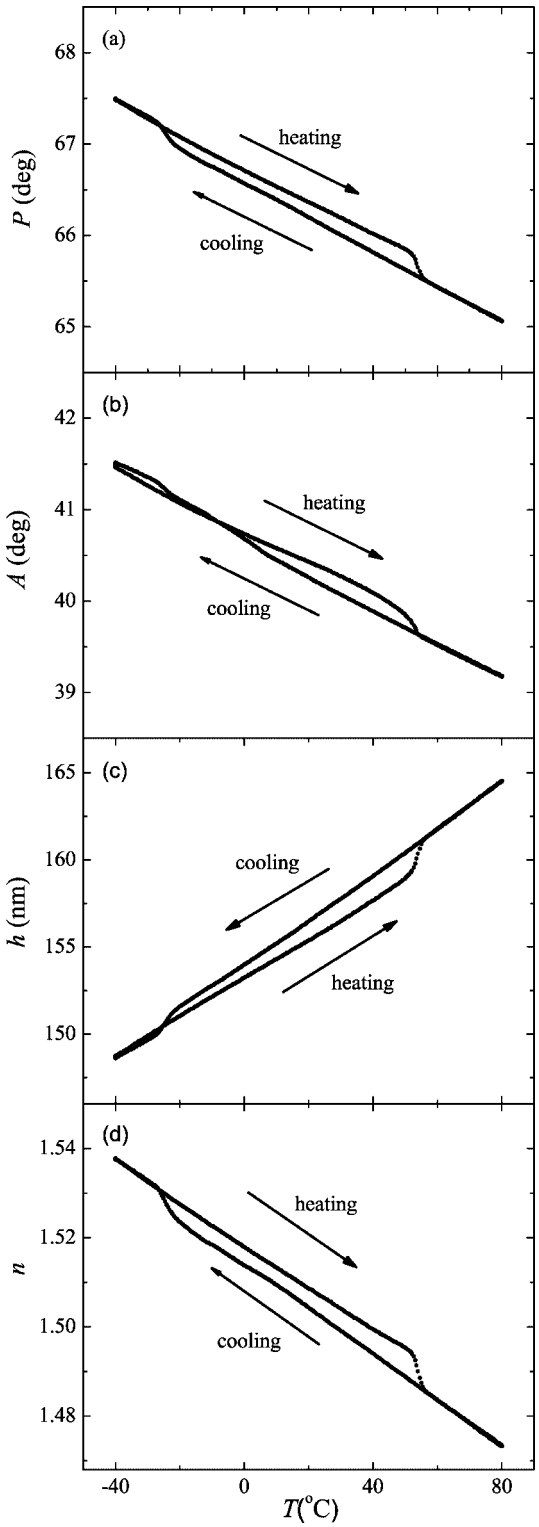

FIGURE 1 The results of a typical ellipsometry experiment for a blended diblock thin film. Measured polarizer, $P(T)$, and analyzer, $A(T)$, angles are plotted as a function of temperature for a fixed rate cooling and heating experiment (a), (b). $P(T)$ and $A(T)$ are used to calculate the corresponding changes in thickness, $h(T)$, and refractive index, $n(T)$, over the course of the experiment (c), (d). Crystallisation and melting transitions are clearly observed around −23 °C and 50 °C.

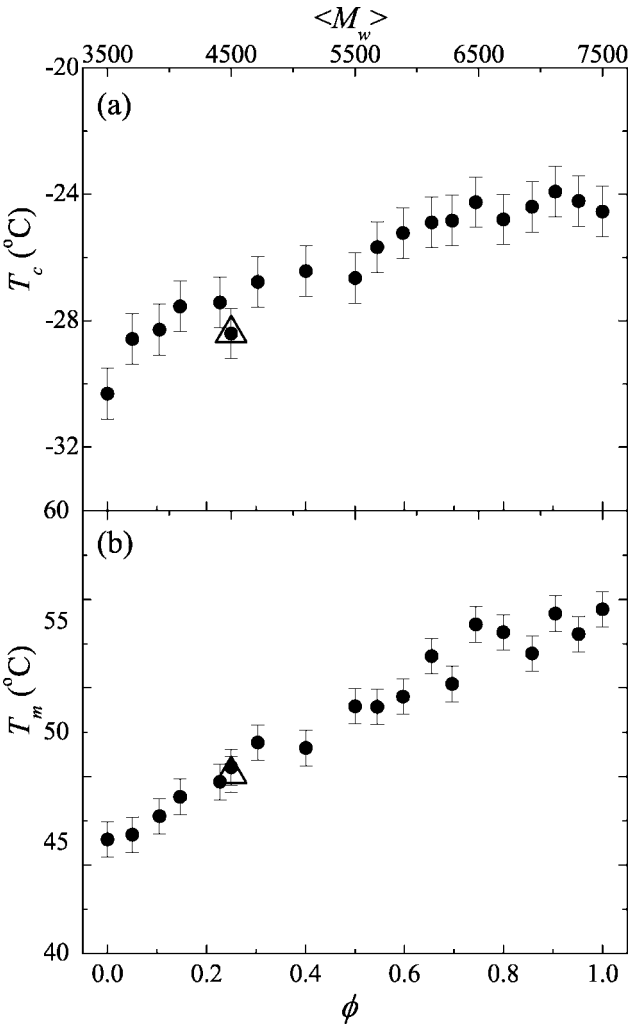

FIGURE 2 (a) Crystallisation, T_c, and (b) melting, T_m, temperatures as a function of blend composition, ϕ, for a series of 3.5 k and 7.5 k diblock blends. The value of ϕ indicates the fraction of 7.5 k component in the blend. The calculated average molecular weight (g/mol) corresponding to the values of ϕ are indicated along the top axis of the plot. The triangle represents the T_c and T_m for a pure 4.5 k diblock film.

displayed in Figure 1. The ellipsometry technique can be used to probe transitions in thin films similar to the use of DSC for bulk materials.

Measurements of the type shown in Figure 1 were repeated for diblock concentrations $0 \leq \phi \leq 1$. In Figure 2, T_c and T_m are shown as a function of the fraction of the large diblock component ϕ. The calculated weight-averaged molecular weight of the PEO component that each blend corresponds to is indicated along the top of the plots. As ϕ is increased, the crystallization temperatures of the blends follow the expected behavior [see Fig. 2(a)]. The pure 3.5 k diblock film ($\phi = 0$, domain radius $R = 5$ nm) displays the lowest value of T_c, with an increasing trend as the blend composition increases to pure 7.5 k ($\phi = 1, R = 14$ nm). The trend in T_c values indicates that the size of the domains increases monotonically between the extreme values. The triangular data point in Figure 2(a) represents T_c for a pure 4.5 k diblock film. This value is in agreement with T_c measured for a 3.5 k/7.5 k blend film with the same average molecular weight of the crystalline block, suggesting that a blend of $\phi = 0.25$ has a similar domain size to the pure 4.5 k film.

We now focus our attention to the melting transition, which also displays a monotonic trend as shown in Figure 2(b). The pure 3.5 k diblock film has the lowest measured T_m, with an increase in T_m as the amount of 7.5 k diblock is increased, up to the maximum value for pure 7.5 k diblock. These results follow from the crystallization data in Figure 2(a). The crystals nucleated at greater supercoolings are formed under larger growth rates, resulting in a lower degree of crystal perfection than crystals formed at higher temperatures. Thus, domains with lower T_c are more unstable to melting and would melt at a lower temperature than domains which nucleate at a higher T_c. Once again, the measured T_m for a pure 4.5 k diblock film, the triangular data point in Figure 2(b), is consistent with the blend film with the same calculated average molecular weight ($\phi = 0.25$). The continuous change in domain size achieved by blending the 3.5 k and 7.5 k diblocks is consistent with the T_c and T_m values measured in Figure 2.

CONCLUSIONS

In this study, we have investigated crystallization and melting temperatures for blends of sphere-forming crystalline-amporphous diblock copolymers. By blending two diblocks with the majority PB block length fixed but different minority PEO block lengths, the size of the spherical domains was varied as a function of blend composition from the smaller sphere radius of the 3.5 k diblock up to the larger radius of the 7.5 k diblock. The changes in sphere size were consistent with a monotonic increase in crystallization and melting temperatures. The changes in melting and crystallization are consistent with, and greatly extend, previous studies on PEO crystallization which have shown a clear relationship between domain size and crystallization temperature.[10] Blending the diblocks provides a simple way to adjust the domain size and ellipsometry proves to be an ideal tool for probing crystallization and melting in nano-confinement.

REFERENCES AND NOTES

1 Vonnegut, B. *J. Colloid Sci.* **1948**, *3*, 563–569.

2 Cormia, R.; Price, F.; Turnbull, D. *J. Chem. Phys.* **1962**, *37*, 1333.

3 Koutsky, J.; Walton, A.; Baer, E. *J. Appl. Phys.* **1967**, *38*, 1832.

4 Frensch, H.; Harnischfeger, P.; Jungnickel, B. *Interface* **1989**, *4*, 20–23.

5 Arnal, M.; Matos, M.; Morales, R.; Santana, O.; Müller, A. *Macromol. Chem. Phys.* **1998**, *199*, 2275–2288.

6 Tol, R.; Mathot, V.; Groeninckx, G. *Polymer* **2005**, *46*, 369–382.

7 Jin, Y.; Hiltner, A.; Baer, E. *J. Polym. Sci. Part B: Polym. Phys.* **2007**, *45*, 1138–1151.

8 Massa, M.; Carvalho, J.; Dalnoki-Veress, K. *Eur. Phys. J. E* **2003**, *12*, 111–117.

9 Massa, M.; Dalnoki-Veress, K. *Phys. Rev. Lett.* **2004**, *92*, 255509.

10 Massa, M.; Carvalho, J.; Dalnoki-Veress, K. *Phys. Rev. Lett.* **2006**, *97*, 247802.

11 Carvalho, J.; Dalnoki-Veress, K. *Phys. Rev. Lett.* **2010**, *PRL 105*, 237801.

12 Kailas, L.; Vasilev, C.; Audinot, J.; Migeon, H.; Hobbs, J. *Macromolecules* **2007**, *40*, 7223–7230.

13 Lotz, B.; Kovacs, A. *ACS Polym. Prepr.* **1969**, *10*, 820–825.

14 Robitaille, C.; Prud'Homme, J. *Macromolecules* **1983**, *16*, 665–671.

15 Loo, Y.-L.; Register, R. A.; Ryan, A. J. *Phys. Rev. Lett.* **2000**, *84*, 4120–4123.

16 Reiter, G.; Castelein, G.; Sommer, J.-U.; Röttele, A.; Thurn-Albrecht, T. *Phys. Rev. Lett.* **2001**, *87*, 226101.

17 Chen, H.; Hsiao, S.; Lin, T.; Yamauchi, K.; Hasegawa, H.; Hashimoto, T. *Macromolecules* **2001**, *34*, 671–674.

18 Zhu, L.; Mimnaugh, B.; Ge, Q.; Quirk, R.; Cheng, S.; Thomas, E.; Lotz, B.; Hsiao, B.; Yeh, F.; Liu, L. *Polymer* **2001**, *42*, 9121–9131.

19 Lorenzo, A.; Arnal, M.; Müller, A.; Boschetti de Fierro, A.; Abetz, V. *Eur. Polym. J.* **2006**, *42*, 516–533.

20 Hobbs, J.; Register, R. *Macromolecules* **2006**, *39*, 703–710.

21 Nojima, S.; Ohguma, Y.; Namiki, S.; Ishizone, T.; Yamaguchi, K. *Macromolecules* **2008**, *41*, 1915–1918.

22 Koneripalli, N.; Levicky, R.; Bates, F.; Matsen, M.; Satija, S.; Ankner, J.; Kaiser, H. *Macromolecules* **1998**, *31*, 3498–3508.

23 Hashimoto, T.; Yamasaki, K.; Koizumi, S.; Hasegawa, H. *Macromolecules* **1993**, *26*, 2895–2904.

24 Mayes, A.; Russell, T.; Deline, V.; Satija, S.; Majkrzak, C. *Macromolecules* **1994**, *27*, 7447–7453.

25 Yamaguchi, D.; Hashimoto, T. *Macromolecules* **2001**, *34*, 6495–6505.

26 Spontak, R. J.; Fung, J. C.; Braunfeld, M. B.; Sedat, J. W.; Agard, D. A.; Kane, L.; Smith, S. D.; Satkowski, M. M.; Ashraf, A.; Hajduk, D. A.; Gruner, S. M. *Macromolecules* **1996**, *29*, 4494–4507.

27 Huang, Y.; Nandan, B.; Chen, H.; Liao, C.; Jeng, U. *Macromolecules* **2004**, *37*, 8175–8179.

28 Takeshita, H.; Gao, Y.; Natsui, T.; Rodriguez, E.; Miya, M.; Takenaka, K.; Shiomi, T. *Polymer* **2007**, *48*, 7660–7671.

29 Shi, A.; Noolandi, J. *Macromolecules* **1994**, *27*, 2936–2944.

30 Hashimoto, T. *Macromolecules* **2002**, *35*, 2566–2575.

31 Papadakis, C.; Mortensen, K.; Posselt, D. Eur. Phys. J. B-Condens. Matter Complex Syst. **1998**, *4*, 325–332.

32 Tanimoto, S.; Ito, K.; Sasaki, S.; Takeshita, H.; Nojima, S. Polym. J. **2002**, *34*, 593–600.

33 Matsen, M.; Bates, F. *J. Chem. Phys.* **1997**, *106*, 2436–2448.

34 Vasilev, C.; Reiter, G.; Pispas, S.; Hadjichristidis, N. *Polymer* **2006**, *47*, 330–340.

35 Huang, Y.; Chen, H.; Hashimoto, T. *Macromolecules* **2003**, *36*, 764–770.

36 Azzam, R. M. A.; Bashara, N. M. Ellipsometry and Polarized Light; North Holland, Amsterdam, 1987.

37 Carvalho, J.; Massa, M.; Dalnoki-Veress, K. *J. Polym. Sci. Part B: Polym. Phys.* **2006**, *44*, 3448–3452.

38 Wang, T.; Dunbar, A. D. F.; Staniec, P. A.; Pearson, A. J.; Hopkinson, P. E.; MacDonald, J. E.; Lilliu, S.; Pizzey, C.; Terrill, N. J.; Donald, A. M.; Ryan, A. J.; Jones, R. A. L.; Lidzey, D. G. *Soft Matter* **2010**, *6*, 4128–4134.

39 Matsen, M. *J. Phys: Condens. Matter* **2002**, *14*, R21.